

Praktikum: P4 Gruppe: 22

☒ **Mo** ☐ **Mi**
Zutreffendes bitte ausfüllen

WS20/21

Namen: Paul Filip useba[at]student.kit.edu

Namen: Janic Beck

Versuch: Tiefe Temperaturen

Betreuer: Daria Gusenkova Durchgeführt am: 18.01.202

Wird vom Betreuer ausgefüllt.

1. Abgabe am: _____

Rückgabe am: _____ Kommentar:

2. Abgabe am: _____

Ergebnis: + / 0 / - Handzeichen: _____

Datum: _____ Kommentar:

Contents

1	Theory & Preparation	1
1.1	Aim of the experiment	1
1.2	Electrical resistance of metals	1
1.3	Semiconductors	1
1.3.1	Intrinsic semiconductor	2
1.3.2	Extrinsic semiconductor	2
1.4	Superconductors	2
1.4.1	Superconductor in magnetic field	3
1.4.2	Ginsburg-Landau Theory (GLAG)	3
2	Experiment & Evaluation	5
2.1	Experimental setup	5
2.2	Copper and Niobium	5
2.3	Superconductivity of Nb	9
2.4	Activation energy of Si	10
2.5	Conclusion	11
	Bibliography	12

1. Theory & Preparation

1.1 Aim of the experiment

The low temperature properties of different solids are determined in the experiment. Especially the electrical resistance of metals, semiconductors and superconductors. We expect a phase shift for the superconductor which requires special consideration.

1.2 Electrical resistance of metals

A simple description with the Drude model can be used for metals. The electrons are accelerated in an electric field and scattered at the atomic cores after a mean free path. It follows for the electrical conductivity:

$$\sigma = \frac{ne^2\tau}{m_e} \quad (1.1)$$

where n is the charge carrier density, τ is the mean free time, and e is the elementary charge. The temperature dependent conductivity follows from the mean free time τ . This is due to the scattering of electrons by phonons and impurities in the lattice. The resistivity is given by $\sigma = \frac{1}{\rho}$ to Matthiessen's rule:

$$\rho = \rho_{ph}(T) + \rho_{im} \quad (1.2)$$

The scattering at impurities is independent of temperature and is reflected in a constant residual resistance. The following temperature dependencies apply to phonon scattering:

- For high temperatures ($T > \Theta_D$, with Θ_D Debye temperature).

$$\rho_{ph} \propto T \quad (1.3)$$

- For low temperatures ($T < \Theta_D$)

$$\rho_{ph} \propto T^5 \quad (1.4)$$

Where for high temperatures, according to Grüneisen-Bornelius, one can determine the Debye temperature with:

$$R_T = 1,17 \frac{R(\Theta_D)}{\Theta_D} T - 0,17 \cdot R(\Theta_D) \quad (1.5)$$

1.3 Semiconductors

Semiconductors are very different from normal conductors like metals. For $T \rightarrow 0$ the valence band is completely filled and the conduction band is empty. One can distinguish between intrinsic and extrinsic semiconductors.

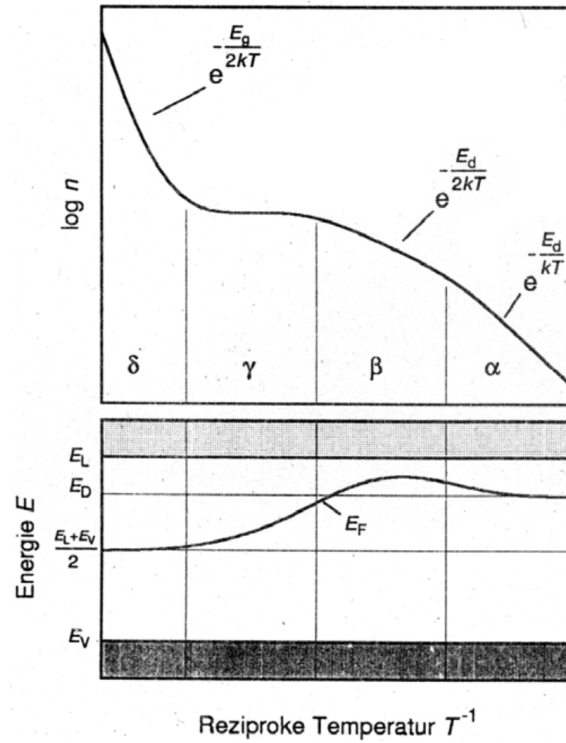


Figure 1.1: Temperature dependent charge carrier concentration in extrinsic semiconductors.

1.3.1 Intrinsic semiconductor

Since neither a full valence band nor an empty conduction band contributes to charge transport, the electrons have to overcome an energy gap E_{gap} to the next band. This is done by thermal excitation, which is obviously temperature dependent. Thus for the electrical conductivity follows:

$$\sigma_{tot} = \sigma_e + \sigma_h = n_i e (\mu_e + \mu_h) \quad (1.6)$$

where n_i corresponds to the electron / hole density and μ to the corresponding mobility. In the end, the following equation is obtained:

$$\sigma_i = C_i \exp\left(-\frac{E_{gap}}{2k_B T}\right) \quad (1.7)$$

Thus, the electrical conductivity approaches the constant C_i asymptotically.

1.3.2 Extrinsic semiconductor

By doping a semiconductor, its conductivity can be strongly increased. In this process impurities of the neighboring main group are added. These atoms either donate electrons (donors) or accept electrons (acceptors) and produce a n/p doped semiconductor. Sub-energy levels are created in the band gap which can be excited more easily. This results in a complicated temperature profile with $\sigma = en\mu$.

1.4 Superconductors

Unlike metals and semiconductors, a superconductor has a critical temperature T_c . Below this temperature the electrical resistance disappears and the superconductor behaves like an ideal conductor. Due to the Meissner-Ochsenfeld effect, the superconductor also behaves like

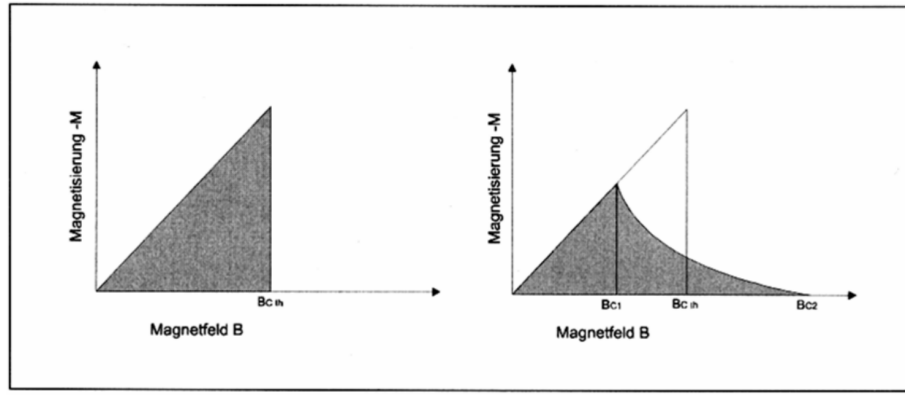


Figure 1.2: Magnetization curve of superconductors 1st kind (left) and 2nd kind (right)

a diamagnet ($\chi = -1$). One can distinguish between metallic and ceramic superconductors. Metallic superconductors usually have lower critical temperatures. These phenomena can be described by the BCS theory. Two electrons form a Cooper pair with spin 1. So they behave like bosons, do not obey the Pauli principle like single electrons and have no total momentum.

$$(\vec{k} \uparrow, -\vec{k} \downarrow)$$

This behavior is explained via the polarization of the atomic lattice by the first electron and the resulting attraction of the second electron. The phonons are the exchange particles of this exchange interaction. The Cooper pairs all occupy the same quantum mechanical state at low temperatures and are therefore firmly correlated. If now an external electric field is applied, all Cooper pairs get the same momentum. However, the individual Cooper pairs cannot exchange momentum with the lattice because they are all in the same state and not all electrons can be scattered simultaneously. This effect describes nothing else than resistanceless charge transport through the lattice. However, the stability is limited by the binding energy of the pair correlation of the Cooper pairs. If the momentum of the Cooper pairs increases by the electric field and thus their energy exceeds the binding energy, the interaction with the lattice starts again. Thus, there is a critical momentum (equivalent to current density) above which the superconductor becomes a normal conductor.

1.4.1 Superconductor in magnetic field

From the critical current density implied above, a critical magnetic field follows immediately. This behavior is described by the Meissner-Ochsenfeld effect. Here, the external magnetic field induces continuous currents at the surface of the superconductor and the external magnetic field is forced out of the inside. However, a small London penetration depth λ exists. One can now distinguish between two types of superconductors:

- superconductors 1st kind show the Meissner effect up to a critical field $B_{c,th}$.
- Superconductors 2nd kind show the Meissner effect up to B_{c1} and then enter the Shubnikov phase up to a field B_{c2} .

1.4.2 Ginsburg-Landau Theory (GLAG)

Considering the problem as a phase transition, one can define an order parameter ϕ near the critical temperature. In our case, this describes the Cooper pair density and accordingly vanishes in the disordered phase for $T > T_c$. If we now develop the free energy density as powers of the order parameter in thermodynamic equilibrium, it becomes minimal. Thus,

all other thermodynamic quantities can be derived such as the critical magnetic field B_{c2} , the Ginzburg-Landau coherence length ξ_{GL} and the London penetration depth λ .

$$\lambda(T) = \lambda(0) \left(1 - \left(\frac{T}{T_C} \right)^4 \right)^{-1/2} \quad (1.8)$$

For the upper critical field B_{c2} , it follows:

$$B_{c2}(T) = \frac{\Phi_0}{2\pi\xi_{GL}^2(T)} \quad (1.9)$$

with flux quantum $\Phi_0 = \frac{h}{2e}$ and GL coherence length ξ_{GL} :

$$\xi_{GL}(T) = \frac{\xi_{GL}(0)}{\sqrt{1 - T/T_c}} \quad (1.10)$$

When $T = 0$, it follows:

$$\xi_{GL}(0) = \left[\frac{-\Phi_0}{2\pi T_c \frac{dB_{c2}}{dT}|_{T_c}} \right] \quad (1.11)$$

and the mean free path l for niobium as normal conductor is given by:

$$\xi_{GL}(0) = \sqrt{39 \text{ nm} \cdot l} \quad (1.12)$$

2. Experiment & Evaluation

2.1 Experimental setup

The cryostat consists of two double-walled shells, so-called glass dewars (see figure *Figure 2.1*). These allow thermal isolation from the room temperature. The outer glass dewar is filled with liquid nitrogen and cooled down to 80 K. To reach lower temperatures, the inner glass dewar is cooled with liquid helium up to 5 K. It also contains the sample cup with three samples: copper (metal), niobium (superconductor) and silicon (pure semiconductor). A superconducting coil is also attached to observe the behavior of niobium at the transition temperature with external magnetic field. A platinum and, from 30 K, a carbon thermomenter are used to measure the temperature, at which the specific resistances are measured.

The observed electrical resistance of copper is shown in Figure 2.2. The observed electrical resistances of niobium and silicon are displayed in Figure 2.3 and Figure 2.4 respectively. For an analysis of the gathered information refer to the following sections.

2.2 Copper and Niobium

The electrical properties of metals with respect to their temperature has been discussed in chapter 1. In the following section, the established theory is compared to the experimentally gathered data from section 2.1.

First and foremost, the high-temperature (≥ 50 K) limit of metals is evaluated. According to Equation 1.5 the resistance should drop off linearly when the conductor is cooled down. This behaviour is indeed mirrored by both copper and niobium. A more precise analysis find the Debye-temperature θ and the Debye-resistance R_θ as listed in Table 2.1.

Both sets of measurements do not conform to literature values ($\theta_{\text{Cu}} = 343$ K, $\theta_{\text{Nb}} = 275$ K). This may be caused by imperfect calibrations of the measured temperature, a bad fitting algorithm or simply measurement errors. In order to put this disagreement between theory and experiment into perspective, Figure 2.2 in addition to measurement data shows a rough estimate of what one would expect from theory based on a Debye-temperature of $\theta = 343$ K.

Table 2.1: Fit parameters for copper and niobium

Material	θ	R_θ
Copper	(266.797 ± 1.591) K	(2.011 ± 0.027) Ω
Niobium	(224.270 ± 4.925) K	(25.137 ± 0.661) Ω

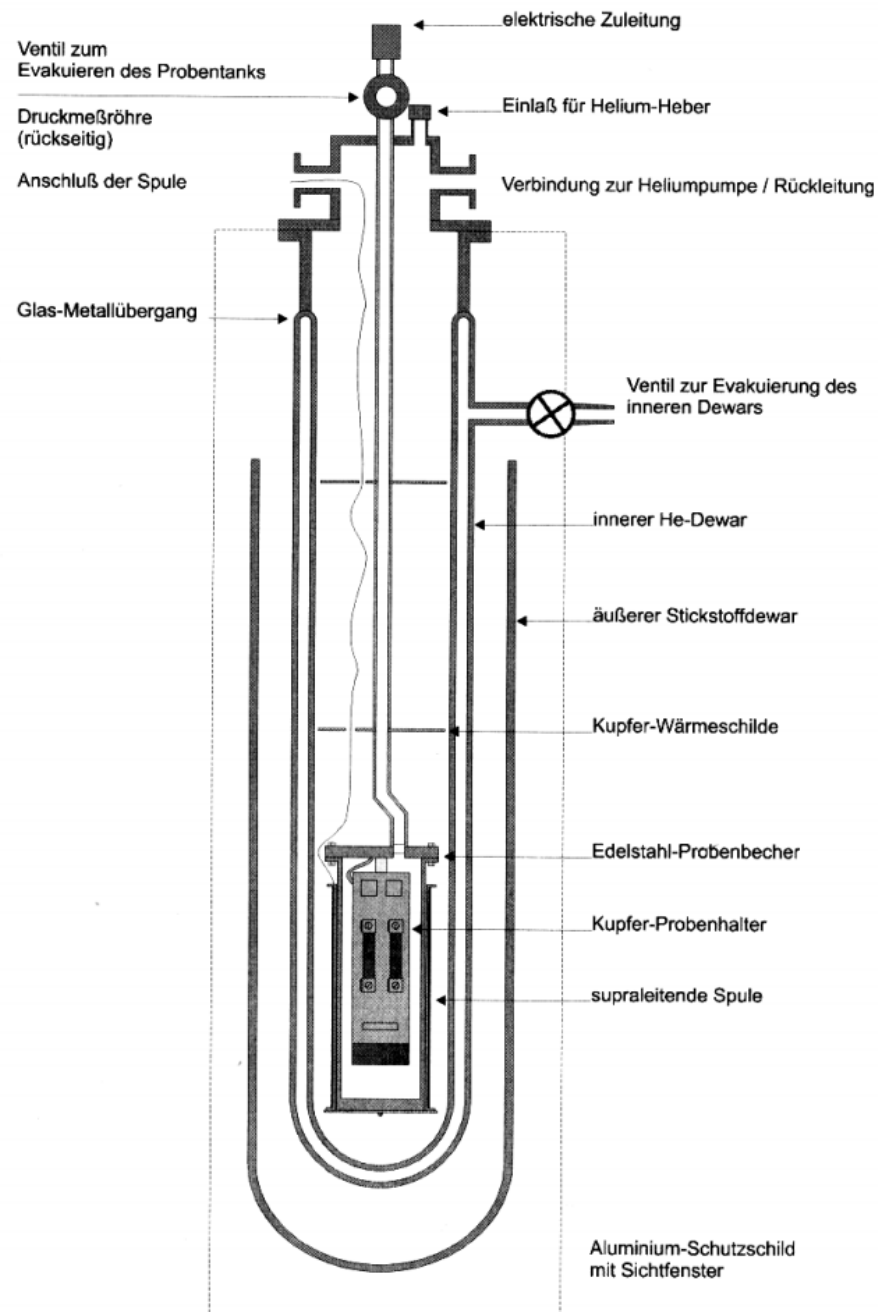


Figure 2.1: Kryostat

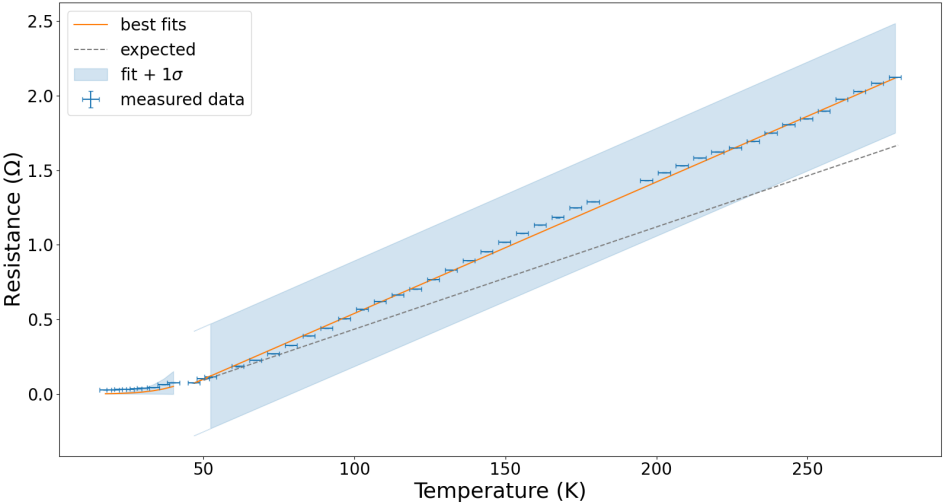


Figure 2.2: Electrical resistance of copper at different temperatures

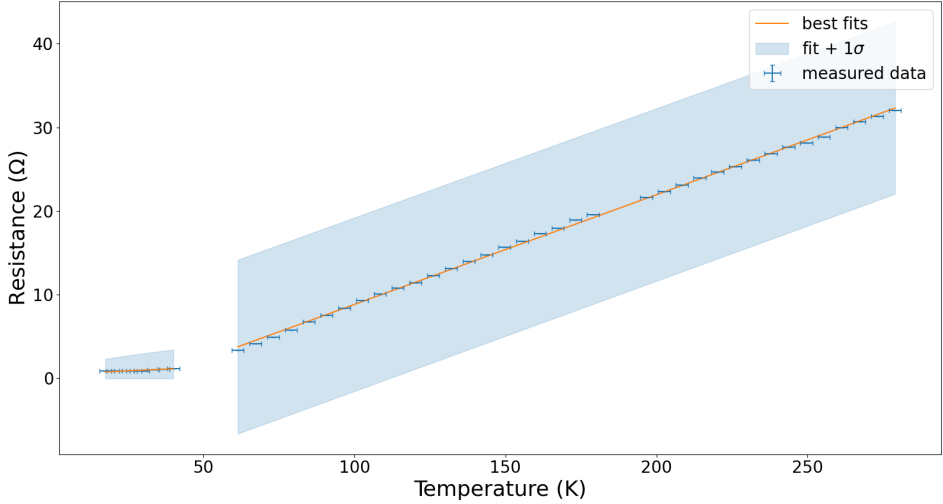


Figure 2.3: Electrical resistance of niobium at different temperatures

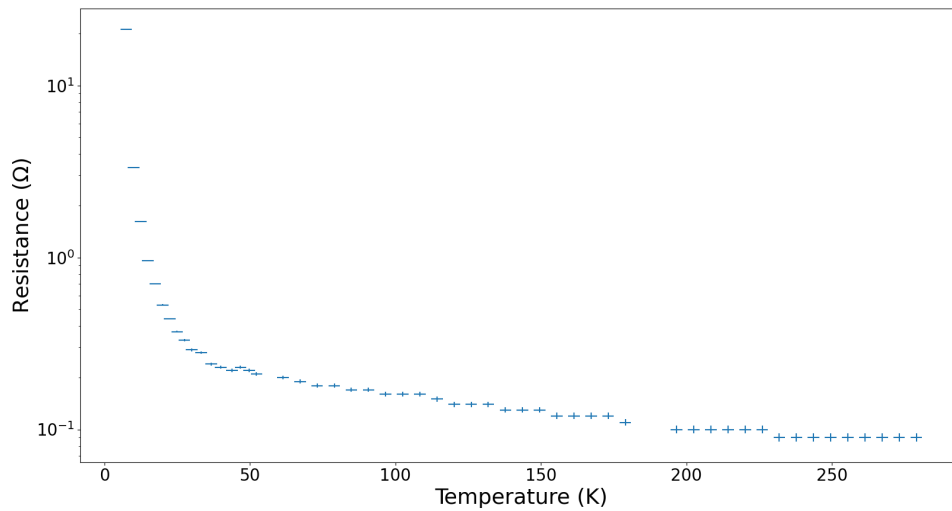


Figure 2.4: Electrical resistance of silicon at different temperatures

In a second part of the analysis, the nonlinear, low-temperature regime is analysed for both conductors. According to the theory layed out in chapter 1, it is expected that the electrical resistance is proportional to T^5 . To test this hypothesis, a polynomial of form $R \propto T^m$ is fitted to the data points found at the low end of the temperature scale (< 50 K). The analysis finds

$$\text{Copper : } m = 4.834 \pm 0.157$$

$$\text{Niobium : } m = 4.40 \pm 0.71$$

While both data sets again do not conform exactly to theory ($m = 5$), a clear hint to the T^5 -behaviour can be extracted from the found results. Furthermore, the resistivity ρ and mean free path μ at low temperatures is evaluated for both copper and niobium are evaluated as explained in the lab manual. The analysis finds the resistivities to be

$$\rho_{\text{Cu}}(4.2 \text{ K}) = (8.2 \pm 2.5) \times 10^{-12} \Omega \text{ m}$$

$$\rho_{\text{Nb}}(12 \text{ K}) = (29.0 \pm 2.5) \times 10^{-10} \Omega \text{ m}.$$

From this, the mean free path can be gathered from its connection with the constant ρl :

$$\mu_{\text{Cu}} = \frac{\rho l_{\text{Cu}}}{\rho_{\text{Cu}}} = (80 \pm 24) \mu\text{m}$$

$$\mu_{\text{Nb}} = \dots = (130 \pm 11) \text{ nm}$$

Lastly, the validity of Equation 1.5 is evaluated via a combined analysis of both copper and niobium data. For this purpose the reduced resistivity $\frac{R}{R_\theta}$ is plotted against the reduced

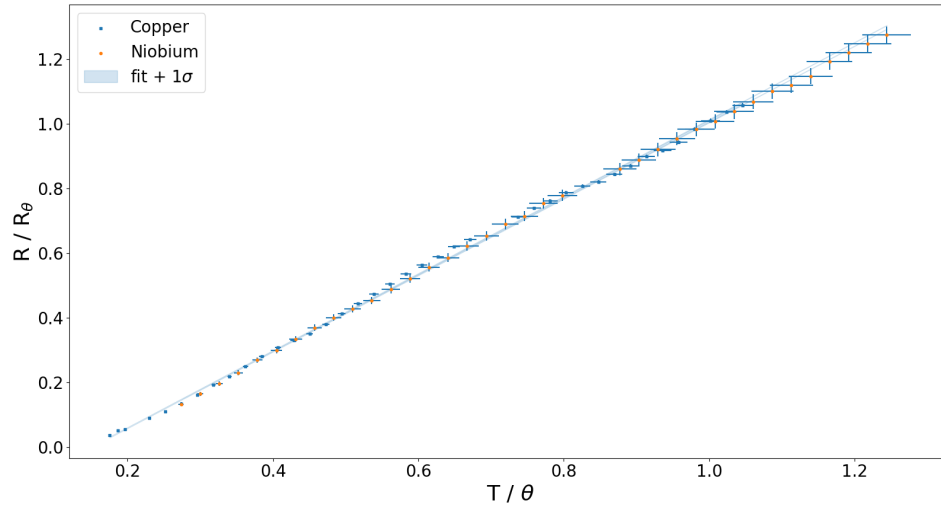


Figure 2.5: Combined analysis of copper and niobium

Table 2.2: Critical temperature measurement values at critical magnetic field

T_c in K	I in A	B_{c2} in T
9,2	0	0
8,99	1,5	0,071895
8,84	3	0,14379
8,74	4,5	0,215685
8,56	6	0,28758
8,45	7,5	0,359475
8,35	9	0,43137
8,25	10,5	0,503265

temperature $\frac{T}{\theta}$. This approach should eliminate possible systematic errors made during the measurement process. A visualisation can be found in Figure 2.5. A linear regression reveals, that both sets of data can be described by a line with parameters

$$\begin{aligned} \text{Slope : } m &= 1.185 \pm 0.006 \\ \text{Intercept : } b &= -0.177 \pm 0.002, \end{aligned}$$

which unsurprisingly resemble the values in Equation 1.5 by a lot. The validity of the Grüneisen-Borellius formula and underlying theory is therefore verified.

2.3 Superconductivity of Nb

With the help of an X-Y plotter, the resistance of niobium is determined as a function of the external magnetic field. The critical temperature is evaluated at the point where the resistance of niobium falls to half of the maximum value. It follows for the different magnetic field strengths:

The relationship between current and magnetic field was taken from the preparation folder

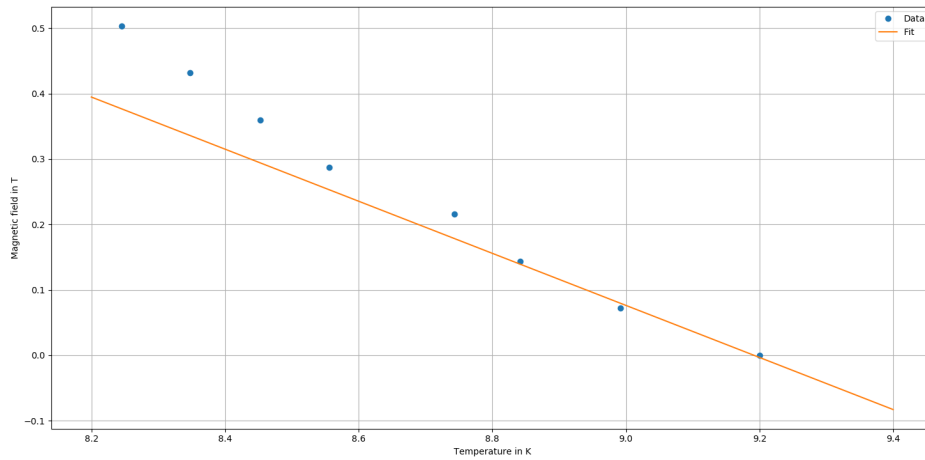


Figure 2.6: Temperature dependency of upper critical field

¹ and the temperature was determined analogously to previous tasks with the carbon thermometer.

In figure *Figure 2.6* it shows, as expected, that the critical temperature decreases with increasing magnetic field. Using a linear fit, the coherence length $\xi_{GL}(0)$ can now be determined to:

$$\xi_{GL}(0) = \left[\frac{-\Phi_0}{2\pi T_c A} \right] \quad (2.1)$$

where A corresponds to the gradient of the straight $f(x) = Ax + b$. Thus, the coherence length is calculated as $\Phi_0 = 2.07 \times 10^{-15} \text{ Vs}$ to:

$$A = (-397.9 \pm 37.8) \frac{\text{mT}}{\text{K}}$$

$$\Rightarrow \xi_{GL}(0) = (9.49 \pm 0.45) \text{ nm}$$

From the coherence length, the mean free path l for niobium can now be obtained via:

$$l = (2.31 \pm 0.22) \text{ nm} \quad (2.2)$$

2.4 Activation energy of Si

The activation energy of Si can be determined from the electrical conductivity σ . For this applies:

$$\sigma = \frac{1}{\rho} = \frac{l}{R \cdot A} \quad \sigma = C \cdot \exp\left(\frac{-E_a}{2k_B T}\right) \quad (2.3)$$

¹Elektrische Leitfähigkeit von Festkörpern bei tiefen Temperaturen im Fortgeschrittenenpraktikum des Physikstudiums von Matthias Klaus Sickmüller, Page 34

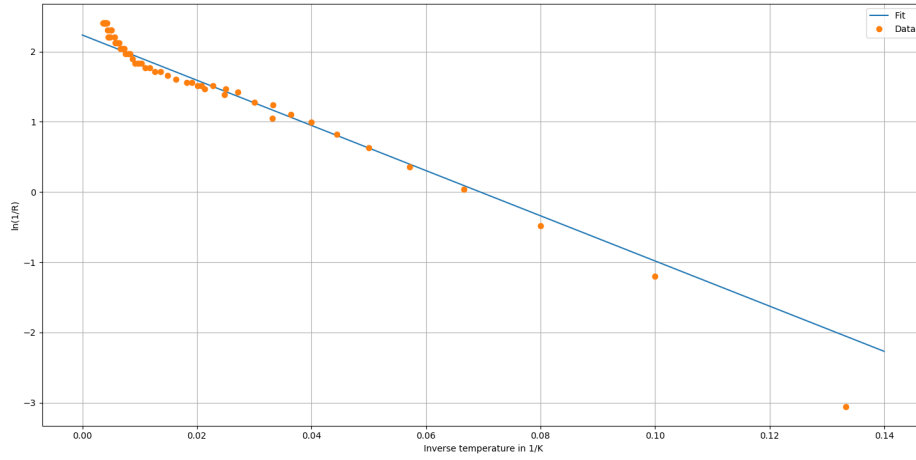


Figure 2.7: Fit for the activation energy

where l is the length and A is the cross-sectional area of the sample. For the silicon semiconductor, it follows:

$$\Rightarrow \ln\left(\frac{1}{R}\right) = \frac{-E_a}{2k_B} \cdot \frac{1}{T} - \ln\left(\frac{l}{AC}\right) \quad (2.4)$$

Therefore, if we plot the natural logarithm of the inverse resistance versus the inverse temperature, we can see a linear relationship at low temperatures. Hence, from the fit $f(x) = Ax + B$, the activation energy can be determined. As for the activation energy with gradient $A = (-32.17 \pm 1.02) \text{ K}$:

$$E_a = -2k_B A \quad k_B = 8.617343 \frac{\text{eV}}{\text{K}} \quad (2.5)$$

$$\Rightarrow E_a = (5.54 \pm 0.18) \text{ meV} \quad (2.6)$$

2.5 Conclusion

Several qualities of different electrical conductors have been tested both qualitatively and quantitatively. While the measurement results overall conform to the theory established in chapter 1, large discrepancies are found when comparing the exact numerical results of e.g. the Curie-temperature of Copper to literature values. Even cross checks between results in this report fail. The mean free path of niobium for example has been calculated in two different ways. The two results differ by a two orders of magnitude. This hints at systematic errors in the analysis. Especially the calibration temperature to the different thermometers is thought to be faulty.

Bibliography